Rotational Resonance Determination of the Structure of an Enzyme–Inhibitor Complex: Phosphorylation of an (Aminoalkyl)phosphinate Inhibitor of D-Alanyl-D-alanine Ligase by ATP†

Ann E. McDermott, F. Creuzet,‡ and R. G. Griffin*

Francis Bitter National Magnet Laboratory and Department of Chemistry, Massachusetts Institute of Technology, Cambridge, Massachusetts 02139

Laura E. Zawadzke, Qi-Zhuang Ye, and Christopher T. Walsh

Department of Biological Chemistry and Molecular Pharmacology, Harvard Medical School, Boston, Massachusetts 02115

Received November 21, 1989; Revised Manuscript Received February 23, 1990

ABSTRACT: We have used a newly developed solid-state NMR method, rotational resonance, to establish the structure of an inhibited complex formed upon reaction of D-alanyl-D-alanine ligase, ATP, and the aminoalkyl dipeptide analogue [1(*S*)-aminoethyl][2-carboxy-2(*R*)-methyl-1-ethyl]phosphinic acid (Ib). Analogue Ib was determined to be an ATP-dependent, slow-binding inhibitor of the D-Ala-D-Ala ligase from *Salmonella typhimurium*, with an enzyme–inhibitor half-life of 17 days at 37 °C. The inhibited complex shows a ^{31}P NMR spectrum which is very different from that which would arise from a mixture of the free inhibitor and ATP. Four well-resolved lines were observed: two (at −8 and −14 ppm) are assignable as the phosphates of ADP, the third is assignable to an inhibitor resonance (at 53 ppm) that shifts by approximately 19 ppm on binding, and the fourth is assignable to a resonance (at −3 ppm) due to a polyphosphate or phosphate ester moiety. At rotational resonance the spectrum shows evidence for strong dipolar couplings between the phosphinate phosphorus and a phosphate ester species. The dipolar coupling between the phosphorus signals at 53 and −3 ppm was measured at rotational resonance by use of numerical simulations of both the line shape of the signal and the profile of magnetization transfer between the two sites. The measured coupling, 1.0 ± 0.2 kHz, indicates that the two species are bridged in a P–O–P linkage, with a P–P through-space distance of 2.7 ± 0.2 Å. This proves that the mechanism of inactivation involves phosphorylation of the enzyme-bound inhibitor by ATP to form a phosphoryl–phosphinate adduct.

In the synthesis of the protective outer peptidoglycan layer, prokaryotes employ several enzymes that prepare and use D-alanine. This layer constitutes one of the rare examples of D-amino acid utilization in biology. Consequently, inhibition of these D-amino acid specific enzymes represents an interesting avenue for antibiotic development (Park, 1958). Conceptually, the first enzyme in this pathway is alanine racemase (Walsh, 1989), which converts L- to D-alanine; the mechanism of inhibition of this enzyme was recently studied by solid-state NMR (Copie et al., 1988). The present study concerns D-Ala-D-Ala[1] ligase, the second enzyme in the pathway, which polymerizes D-alanine to form the dipeptide in an ATP-dependent reaction. Subsequently, the dipeptide is coupled with uridine 5′-diphosphate–*N*-(acetylmuramyl)-L-Ala-D-Glu-*meso*-diaminopimelic acid to yield the pentapeptide UDP–*N*-(acetylmuramyl)-L-Ala-D-Glu-*meso*-DAP-D-Ala-D-Ala, a crucial component for cell wall peptidoglycan. To facilitate characterization of the enzyme, the D-Ala-D-Ala ligase from *Salmonella typhimurium* has recently been cloned, sequenced, overproduced, and purified to homogeneity (Daub et al., 1988; Knox et al., 1989).

Three potent inhibitors of D-Ala-D-Ala ligase have been prepared (Parsons et al., 1988) that contain a phosphinate moiety in a position analogous to the amide carbonyl in the dipeptide (Ia–c); the parent compound is the (aminoalkyl)-phosphinate [1(*R*,*S*)-aminoethyl][2-carboxy-2(*R*,*S*)-alkyl-1-ethyl]phosphinic acid (I). After incubation in the presence

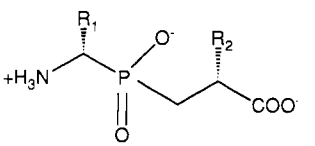

R1 R2

Ia (S)-methyl (R,S)-heptyl

Ib (S)-methyl (R)-methyl

Ic (S)-methyl (R)-thiomethyl

of ATP and subsequent 24-h dialysis, these three analogues, 1(*S*)-methyl 2(*R*)-(methylthio), 1(*S*)-methyl 2(*R*,*S*)-heptyl, and 1(*S*)-methyl 2(*R*)-methyl, exhibit 96, 53, and 93%, respectively, of the inhibition of the relatively crude preparation of Gram-positive *Streptococcus faecalis* ligase (Parsons et al., 1988). Thus, the two inhibitors with the less bulky methyl and methylthio substituents in the R_2 position apparently form stable, long-lived inhibited enzyme complexes, which are ideal

† This work was supported in part by grants from the National Institutes of Health (GM-24305 and RR-00995) and from the National Science Foundation (PCM 8308969). A.E.M. was supported by a postdoctoral fellowship from the American Cancer Society (PF-3283).

‡ Present address: Laboratoire de Physique des Solides, Bat. 510, Université Paris-Sud, 91405 Orsay Cedex, France.

[1] Abbreviations: ADP, adenosine 5′-diphosphate; ATP, adenosine 5′-triphosphate; D-Ala-D-Ala, D-alanyl-D-alanine; DAP, diaminopimelic acid; HEPES, *N*-(2-hydroxyethyl)piperazine-*N*′-2-ethanesulfonic acid; LDH, lactate dehydrogenase; MAS, magic angle spinning; NADH, nicotinamide adenine dinucleotide hydride; PEI, poly(ethylenimine); PK, pyruvate kinase; PEP, phosphoenolpyruvate; NMR, nuclear magnetic resonance; UDP, uridine 5′-diphosphate.

0006-2960/90/0429-5767$02.50/0

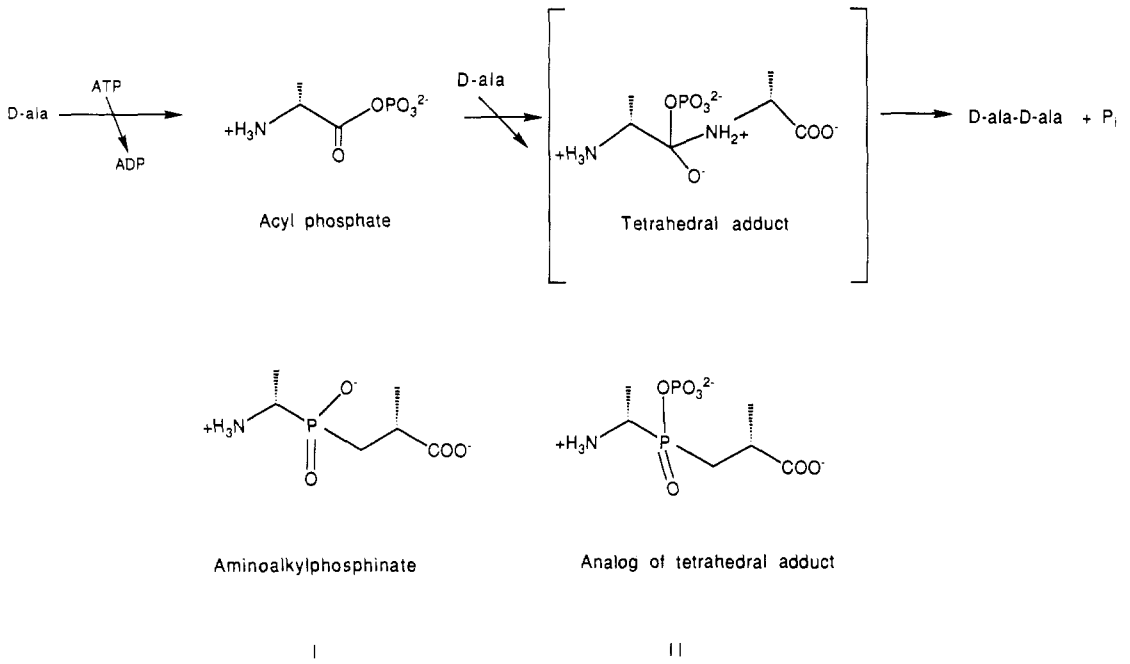

FIGURE 1: Substrate catalysis by D-Ala-D-Ala ligase putatively proceeds through a tetrahedral intermediate as shown. We propose that inhibitor I becomes phosphorylated in the enzyme active site to produce species II, which mimics the tetrahedral transition state. The inactivated enzyme complex would then consist of ADP and a phosphoryl phosphinate inhibitor species (II).

candidates for spectroscopic characterization.

In our laboratories, the 1(*S*)-methyl 2(*R,S*)-heptyl analogue (Ia) has been characterized as an ATP-requiring, *slow-binding* inhibitor of D-Ala-D-Ala ligase purified from Gram-negative *S. typhimurium* (Duncan & Walsh, 1988). Slow-binding inhibitors are often characterized by a rapid, reversible binding step, followed by a rather slow, sometimes kinetically irreversible step that causes the overall binding behavior to appear slow. A simplified mechanism is illustrated in eq 1 for D-

$$E + I \underset{K_i}{\overset{ATP}{\rightleftharpoons}} E\cdot I\cdot ATP \underset{k_4}{\overset{k_3}{\rightleftharpoons}} E^*\cdot I\text{-}P\cdot ADP \xrightarrow{k_{irrev}} E + I + ADP + P_i \quad (1)$$

fast; slow; irreversible

Ala-D-Ala ligase inhibition (Morrison & Walsh, 1988). This slow step has generally been assumed to be either a chemical reaction or an enzyme conformational change (or both). It is this step that makes these inhibitors appealing candidates for antibiotics, since it renders them less subject to substrate competition. The role of ATP for inhibition may parallel that for substrate chemistry; as is generally true for amide bond forming enzymes, during substrate catalysis the ATP presumably phosphorylates the D-alanyl carbonyl to generate a good leaving group. It was thus proposed from the kinetic characterization of Ia that the ligase phosphorylates the inhibitor, resulting in a phosphoryl phosphinate moiety which mimics the tetrahedral transition state of normal enzyme catalysis (Figure 1). Upon heat treatment of the inhibited enzyme complex, ATP, ADP, and inorganic phosphate were released, leading to the assumption that such a phosphoryl–phosphinate complex is hydrolytically unstable (Duncan & Walsh, 1988).

An analogous reaction has been shown for another amide bond forming enzyme, glutamine synthetase, which is inhibited by methionine sulfoximine in an ATP-dependent reaction (Ronzio et al., 1969; Manning et al., 1969). In that work, stoichiometric amounts of ADP and methionine sulfoximine phosphate are released from the enzyme upon heat treatment (Ronzio et al., 1969). Similarily, the glutamine synthetase inhibitor phosphinothricin requires ATP for time-dependent inactivation and is also *proposed* to form a phosphoryl phosphinate moiety which hydrolyzes upon release from the enzyme (Colanduoni & Villafranca, 1986). Kinetic studies with glutamine synthetase and several α- and γ-substituted phosphinothricins are consistent with an inhibition mechanism involving phosphinothricin phosphorylation, followed by irreversible release of the inhibitor from the enzyme (Logusch et al., 1989). Although a stable methionine sulfoximine phosphate derivative can be isolated following glutamine synthetase inhibition, the actual occurrence of a *phosphoryl phosphinate* species, following inhibition of either glutamine synthetase inhibition by phosphinothricin or D-Ala-D-Ala ligase inhibition by (aminoalkyl)phosphinic acid, has yet to be clearly established. In addition, none of these inhibitors has yet been shown to be phosphorylated *in the active site.*

Intermediate II shown in Figure 1 would be an excellent candidate for in situ detection by solid-state NMR. The various species involved, ATP, ADP, the phosphinate, and the putative phosphoryl phosphinate, should exhibit diagnostic isotropic chemical shifts and shift anisotropies. In addition, the strong dipolar coupling expected between an oxo-bridged pair of phosphorus atoms should be detectable in solid-state NMR. If present, this coupling, unlike the indirect dipolar or *J* coupling, provides a mechanism for accurate bond distance determination.

Recently, a new method has been developed for measuring homonuclear dipolar couplings, and therefore internuclear distances in amorphous solids. This method is based upon MAS NMR, which utilizes cross polarization (Pines et al., 1973) and magic-angle spinning (Andrew et al., 1958; Lowe, 1959) with proton decoupling (Schaefer & Stejskal, 1976) to achieve high-resolution NMR in amorphous solids. A review of these techniques and their utility for studies of large proteins has recently appeared (Griffin et al., 1988). In general, dipolar couplings between two $I = {}^1/_2$ species would be averaged by sample spinning (Mariq & Waugh, 1979). However, at a condition referred to as *rotational resonance*, in which $\Delta = n\omega_r$, a reduced form of the homonuclear dipolar coupling reappears (Andrew et al., 1963, 1966; Raleigh et al., 1987, 1988;

Columbo et al., 1988). Here Δ is the difference in isotropic shifts, ω_r is the spinning speed, and n is a small integer. The consequences of reintroducing this coupling in an isolated spin pair are both experimentally dramatic and theoretically calculable, making it an appealing method for determining through-space homonuclear distances (Raleigh et al., 1989). From this work two useful methods for bond distance measurements have resulted. In the case of directly bonded atoms, the couplings for the low-order resonances ($n < 3$) may be sufficiently strong that structure appears in the line shape, which can be simulated to obtain the internuclear distance. However, when the dipolar coupling is smaller than approximately 500 Hz (corresponding to $r > 3.3$ Å for ^{31}P), the line-shape effects are small. In this case, bond distance measurements often may be done with magnetization-transfer experiments at rotational resonance. In these experiments, the signal from one member of the pair is selectively inverted, and magnetization exchange with the second is driven coherently by the sample rotation. The time course of this exchange, which is rapid compared with T_1 and spin-diffusion processes, is then measured and simulated to determine the internuclear distance. This latter approach has been used to measure ^{13}C–^{13}C distances up to 5.0 Å in small molecules. In bacteriorhodopsin, a protein with an effective molecular mass of 35 kDa, a distance of 4.2 Å has been measured, despite the presence of a large natural abundance ^{13}C background (F. Creuzet, A. McDermott, R. Gebhardt, J. Herzfeld, J. Lugtenburg, and R. Griffin, unpublished results).

In the present study we employ both line-shape and magnetization-transfer methods to measure the dipolar coupling between the phosphinate and three phosphate species in the D-Ala-D-Ala ligase–inhibitor complex. The methods have permitted an unambiguous demonstration that the phosphinate slow-binding inhibitor is phosphorylated in the active site of the ligase by ATP. The phosphorylated inhibitor has a P–P distance in the P–O–P linkage of 2.7 ± 0.2 Å. Rotational resonance effects are not observed with the other two resonances assigned as ADP peaks, indicating that both ^{31}P atoms of the ADP are more than 5 Å from the phosphinate phosphorus.

Experimental Procedures

Materials. The inhibitor [1(*S*)-aminoethyl][2-carboxy-2-(*R*)-methyl-1-ethyl]phosphinic acid was a generous gift from Dr. A. A. Patchett, Merck Research, Rahway, NJ. The material was resuspended as an aqueous stock to approximately 10 mM. A racemic mixture of the same inhibitor (*S,S*, *R,R*, *S,R*, and *R,S*) was synthesized in our laboratory as described previously (Parsons et al., 1988). The ^{13}C NMR spectra of the racemic mixture suggested that the ratio of isomers in the otherwise pure preparation is approximately 1:1:1:1.

ATP, NADH, D-alanine, and PEI–cellulose plates were from Sigma (St. Louis, MO). Lactate dehydrogenase (LDH), pyruvate kinase (PK), and phosphoenolpyruvate (PEP) were from Boehringer Mannheim Biochemicals (Indianapolis, IN). Bradford reagents were from Bio-Rad (Richmond, CA) and used according to the manufacturer's instructions for protein determinations. A 50-mL stirred ultrafiltration cell and Diaflo PM30 membranes were purchased from Amicon (Danvers, MA). Additional materials for stoichiometry determinations included [U-^{14}C]adenosine 5′-triphosphate (560 mCi/mmol), [γ-^{32}P]ATP (>5000 mCi/mmol), and liquid scintillation fluid from Amersham (Arlington Heights, IL). XAR-5 film for autoradiograms was purchased from Kodak (Rochester, NY). Radioisotopes were counted with a Beckman LS-1801 instrument.

Enzyme Preparation and Assay. Plasmid-encoded D-Ala-D-Ala ligase was purified from *S. typhimurium* DB7000/pDS4 as described in Daub et al. (1988) for use in kinetic analyses. Stocks of the enzyme were stored at either 0.64 or 7 mg/mL in 50% glycerol stock solutions at −20 °C; both stocks maintained a specific activity of 16 μmol min^{-1} mg^{-1} throughout storage life. D-Ala-D-Ala ligase was prepared in large quantities for NMR characterization as described in Knox et al. (1989) from a *tac* overexpression system in *Escherichia coli* and was stored as the lyophilized powder at −20 °C.

Analytical Methods. D-Ala-D-Ala ligase activity was assayed spectrophotometrically on a Gilford 260 spectrophotometer by a PK–LDH coupled enzyme assay, which measures ATP production (Daub et al., 1988). ATP and ADP optical absorption spectra were recorded on a Hewlett-Packard 8452A diode array spectrophotometer.

Inactivation Kinetics. The initial and slow-binding kinetic parameters were determined as described in Duncan and Walsh (1988). The regain of catalytic activity for fully inhibited enzyme was monitored over several days as follows: 30 μL of D-Ala-D-Ala ligase (7 mg/mL), 20 μL of [1(*S,R*)-aminoethyl][2-carboxy-2(*S,R*)-methyl-1-ethyl]phosphinic acid (50 mM), 20 μL of ATP (100 mM), 100 μL of 2× assay buffer (100 mM HEPES, pH 7.8, 20 mM $MgCl_2$, 20 mM KCl), and 30 μL of H_2O were combined and incubated for 2 h at 37 °C. In separate experiments, the ATP was uniformly labeled with ^{14}C (93 mCi/mmol) or γ-labeled with ^{32}P (266 mCi/mmol). The inhibited enzyme was subjected to gel filtration on the fast-desalting column in the Pharmacia FPLC system to remove excess unbound ATP and inhibitor. For the nonradioactive trials, fractions that contained protein were pooled, stored at 37 °C, and assayed over 1 week, until the activity of the previously inhibited enzyme returned to 100% of that of a control sample. (The control sample was prepared in the same way, except with water replacing the inhibitor during the incubation.) The rate of catalytic activity regain, k_{rgn}, was determined from a plot of ln $[100(1 - v/v_s)]$ vs time, where v = velocity at time t and v_s = velocity of the control sample. For the [1(*S,R*)-aminoethyl][2-carboxy-2(*S,R*)-methyl-1-ethyl]phosphinic acid inhibitor, the k_{rgn} was determined to be 4.82×10^{-7} s^{-1}, yielding a $t_{1/2}$ of 16.6 days.

Stoichiometry of ATP and ADP Binding. From the method above, the binding of the radiolabeled ATP to inhibited D-Ala-D-Ala ligase was readily determined. Following the gel filtration step, protein-containing fractions were assayed for activity loss and protein concentration. These fractions were concentrated, heat-denatured, spotted on PEI–cellulose plates, and developed in 1 M KH_2PO_4, pH 3.5. Spots corresponding to radioactive ATP, ADP, or HPO_4^{2-} were excised and counted. ^{14}C-Labeled enzyme produced two spots in the ratio of 24% ATP and 76% ADP. γ-^{32}P-labeled enzyme produced two spots corresponding to 24% ATP and 76% HPO_4^{2-}. The error was determined to be ±3% for each value. Enzyme activity after inhibition, gel filtration, and concentration was always less than 0.5% of the uninhibited enzyme specific activity. The stoichiometry of ^{14}C label/enzyme was 0.83 ± 0.1.

Inhibition of Ligase by [1(S,R)-Aminoethyl][2-carboxy-2(S,R)-methyl-1-ethyl]phosphinic Acid and Lyophilization of the Enzyme–Inhibitor Complex for NMR Analysis. The following components were combined: 5.0 mL of D-Ala-D-Ala ligase (approximately 30 mg), 2.0 mL of ATP (0.1 M), 0.46 mL of [1(*S,R*)-aminoethyl][2-carboxy-2(*S,R*)-methyl-1-ethyl]phosphinic acid (50 mM), 2.44 mL of H_2O, and 10.0 mL of 2× assay buffer. The solution was mixed gently and incubated at 37 °C for 2 h. The enzyme–inhibitor solution

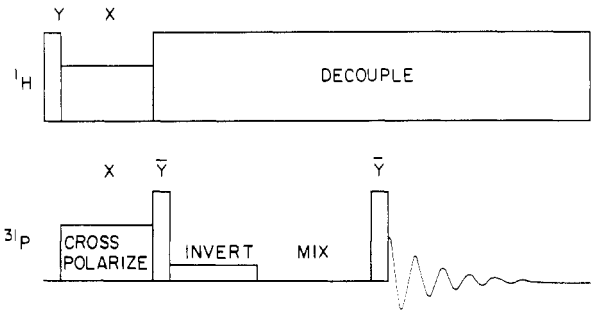

FIGURE 2: NMR pulse sequence used to measure magnetization transfer at rotational resonance. ^{31}P magnetization is developed by cross polarization with the protons and stored along the z axis. Selective inversion of one site (the X–O–PO_3^{2-} at −3 ppm) could then be accomplished with a weak pulse on resonance (t_π = 160 μs). This selectively inverted state is then allowed to evolve for various increments up to 5 ms while the spinning speed was matched to the rotational resonance condition, $\omega_r = \Delta$ (7.167 kHz for the ^{31}P pair of interest). Observation of the evolved state is accomplished by restoring the phosphorus ^{31}P magnetization back to the x–y plane.

(approximately 20 mL) was diluted with 30 mL of 1× assay buffer (a 1:1 dilution of the 2× assay buffer) at 4 °C. This solution was concentrated in the 50-mL Amicon ultrafiltration unit. In order to remove excess ATP and free inhibitor, two additional 40-mL aliquots of 1× assay buffer and then two additional 40-mL aliquots of H_2O were added, and the solution was concentrated after each addition. The enzyme–inhibitor solution after this washing procedure (15-mL volume) was lyophilized. The majority of the enzyme–inhibitor powder was transferred to another container for subsequent ^{31}P solid-state NMR analysis. The remaining material from the walls of the lyophilization flask was resuspended with 5 mL of water. Enzyme activity measurements revealed that enzyme–inhibitor following incubation, following the washing procedure in the Ultrafiltration cell, and following lyophilization exhibited 0.3, 0.4, and 4% of the uninhibited enzyme's specific activity, respectively.

NMR. MAS spectra were collected on a home-built spectrometer operating at a proton frequency of 317 MHz and a ^{31}P frequency of 128.6 MHz. A home-built probe was used, with a stator and rotors from Doty Scientific Inc. (Columbia, SC), capable of spinning to speeds greater than 12 kHz. Typical ^{1}H and ^{31}P 90° pulse lengths were 3 and 4.5 μs, respectively. Recycle delays were 3 s, and optimal cross-polarization times were 0.5 ms for the enzyme and the free inhibitor and 5 ms for ATP. We note that when observing ^{31}P MAS signals in solids spinning at speeds above 5 kHz, unusually sharp cross-polarization matching conditions can occur. Spectra were recorded at room temperature.

Principal values of the shift tensors of ATP, the free heptyl inhibitor, Ia, and the protein-bound species were extracted by computer simulation of the rotational sideband spectrum (Herzfeld & Berger, 1980).

The magnetization-transfer experiments employed the pulse sequence illustrated in Figure 2 (Raleigh et al., 1988). ^{31}P magnetization is prepared in the x–y plane according to standard cross-polarization techniques (Pines et al., 1973) and stored along the z axis with a Y pulse; subsequent selective inversion of one site (the X–O–PO_3 at −3 ppm) was accomplished with a weak on-resonance pulse (t_π = 160 μs). This selectively inverted state is then allowed to evolve with proton decoupling for various time increments with the spinning speed matched to the difference in chemical shifts (7.167 kHz for the ^{31}P pair of interest in this work). Detection of the evolved state was afforded by flipping the phosphorus magnetization back to the x–y plane.

Analysis of the magnetization-transfer data, such as that displayed in Figure 6, involved measuring the peak intensities for the pair at rotational resonance as a function of the mixing time, normalizing the intensity to the initial value, and computing the difference. These values are plotted in Figure 7 along with numerical simulations assuming P–P distances of 2.5 and 2.9 Å.

The algorithms involved in numerical simulations of both the magnetization-transfer rates and the line shape at rotational resonance are described elsewhere (M. H. Levitt, D. P. Raleigh, F. Creuzet, and R. G. Griffin, unpublished results). Parameters involved in the simulations, the bond length determination, and its precision are described under Discussion.

Results

Kinetic Characterization. The inhibition of D-Ala-D-Ala ligase by Ib exhibited slow-binding behavior and showed complete loss of activity. In the presence of ATP and 20 mM D-Ala, the rate constant for enzyme inactivation, k_{inact} = 0.293 s^{-1}, corresponds to a $t_{1/2}$ of inactivation of 2.4 s. The initial K_i for methyl inhibitor Ib binding to ligase is 140 μM (as compared to heptyl inhibitor Ia, which has a K_i = 1.2 μM). As described under Experimental Procedures, the k_{rgn} was determined to be 4.82 × 10^{-7} s^{-1}, yielding a $t_{1/2}$ of 17 days at 37 °C.

Chemical Analysis. ATP is required for the time-dependent inhibition of D-Ala-D-Ala ligase by phosphinic acid inhibitor Ib. ATP and its cleavage products, ADP and P_i, remaining on the enzyme–inhibitor complex were quantitated with radiolabeled ATP. The enzyme was inhibited with Ib in the presence of [^{14}C]ATP and produced two radiolabeled products upon heat denaturing, in the ratio of 24% ATP and 76% ADP. The stoichiometry of ^{14}C label/enzyme was 0.83 ± 0.1. Similarily, the use of γ-^{32}P-labeled ATP during inhibition resulted in 24% ATP and 76% P_i product.

Solid-State NMR. Upon binding ATP and inhibitor Ib to D-Ala-D-Ala ligase, four sharp phosphorus resonances were clearly visible in the solid-state NMR spectrum, together with a small underlying broad component. Spectra taken at a spinning speed $\omega_r/2\pi$ = 10.8 kHz (Figure 3, top panel) allowed unambiguous determination of the number of lines and their isotropic shifts. Spectra obtained at 5.5 kHz (Figure 4) and 5.0 kHz (data not shown) display numerous sidebands and facilitate determination of the chemical shift tensors. Table I lists the isotropic and anisotropic chemical shifts for the four enzyme-bound ^{31}P species as well as for the unbound inhibitors (Ia and Ib) and of the magnesium bipyridylamine salt of ATP (Cini et al., 1984).

The isotropic chemical shifts of the four bound species are clearly different from those of the reactants, and assignment of the four peaks is relatively straightforward. The resonance at +53 ppm must be the phosphinate inhibitor and is significantly shifted from its free form, which resonates at +34 ppm. The dependence of the chemical shift of the free inhibitors, Ia and Ib, on solvent was explored (data not shown). In aqueous or ethanolic solutions the isotropic value did not vary from that determined in the solid state by more than 3 ppm. In addition, the isotropic values for the two compounds (Ia and Ib) are in close proximity (Table I). Thus, the large change in shift on binding is unlikely to be due to environmental effects but rather reflects a change in chemical bonding. There is no well-resolved resonance in the typical range for the β-line of ATP, consistent with the fact that chemical determinations suggest hydrolysis of ATP to ADP. The two lines farthest upfield (−14 and −8 ppm) agree well with the solution isotropic shifts for the α- and β-phosphates in ADP

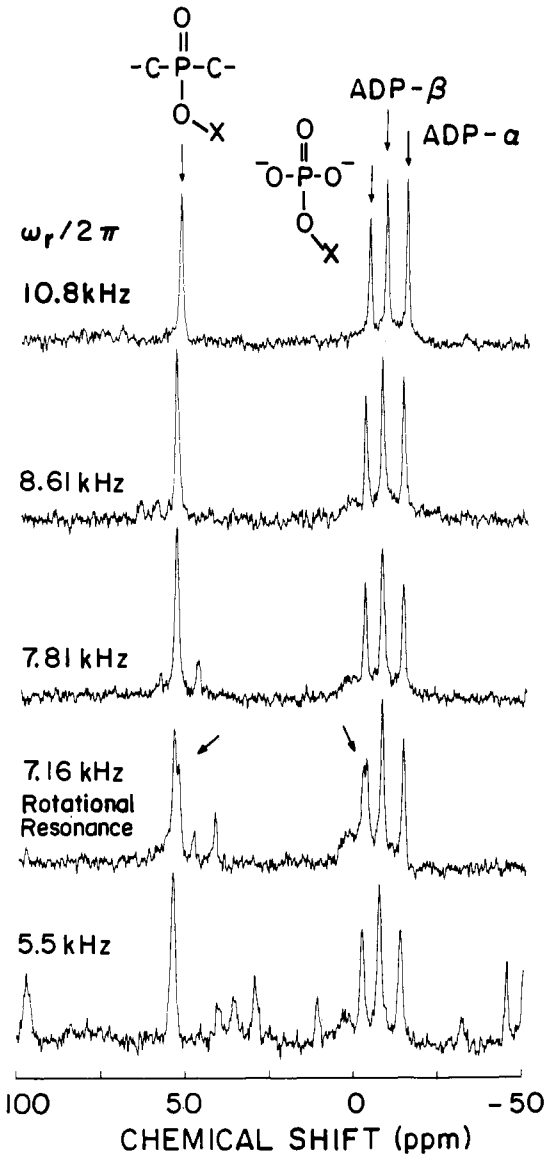

FIGURE 3: MAS spectra of the inhibited complex as a function of spinning speed, ω_r. The speeds were chosen so as to satisfy the rotational resonance condition for the inhibitor and each of the resonances in the phosphate region, in turn. In addition, spectra taken at speeds well above (10.8 kHz) and well below (5.5 kHz) the rotational resonance conditions are shown. A splitting in the peaks due to the inhibitor and the phosphate species at −3 ppm is clearly observable *only* when the speed is adjusted to the isotropic chemical shift difference between the inhibitor and the phosphate ester species, indicating a strong dipolar coupling between the two.

(respectively), and the remaining resonance (−3 ppm) is at a position expected for a polyphosphate or an organic ester of phosphate. On the basis of its spectral characteristics and chemical analysis, the broad underlying component is likely to be ATP in a heterogeneous environment.

The anisotropic chemical shifts of the four sites are also consistent with the above assignments. The overall breadths, δ, of the tensors of the ADP α- and β-sites are similar to those of the phosphates in ATP (see caption for Table I where δ is defined). The dramatic movement in the isotropic shift of the inhibitor is associated primarily with the σ_{22} element of the tensor. The remaining unidentified phosphate at −3 ppm has an overall tensor breadth of δ = 94 ppm. This large value of δ is consistent with a phosphate ester or a polyphosphate, while free phosphate would have a breadth considerably less than that observed. Thus, analysis of the isotropic and anisotropic shift values of the bound species is suggestive, but not conclusive, proof of phosphorylation of the inhibitor.

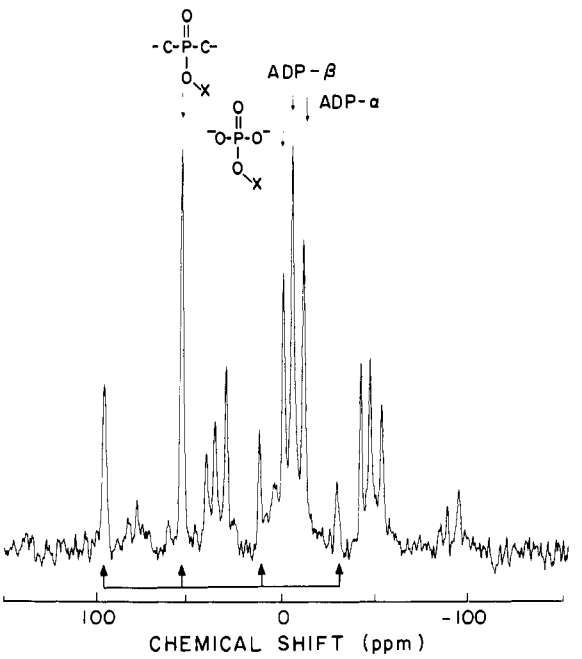

FIGURE 4: MAS spectrum of the inhibited complex at 5.5 kHz, showing the sideband patterns that were simulated to generate the chemical shift tensor parameters in Table I. The centerbands for the four species are labeled from above; a system of arrows below the spectra connects the centerband and family of sidebands for the phosphinate inhibitor. Each of the three peaks in the phosphate region is similarly flanked by several sidebands (not indicated by arrows).

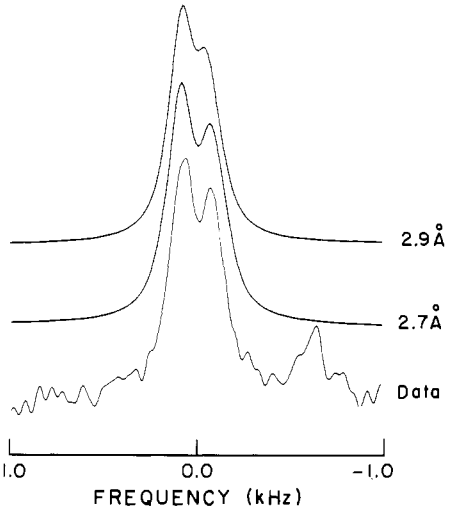

FIGURE 5: Expanded view of the splitting seen at 7.167 kHz which is approximately at rotational resonance for the phosphinate and the phosphate ester (bottom spectrum), together with two simulated spectra. In the data, the feature at approximately −0.6 kHz is a −1 sideband from the β-ADP peak. The simulations involve a dipolar coupling of 1 kHz, corresponding to a P–P distance of 2.7 Å (middle), and a coupling of 800 Hz, corresponding to 2.9 Å (top). Using P–P distances of 2.6–2.7 Å, we obtained excellent agreement with the measured spectrum. The 2.9-Å simulation shown is the optimal fit for that bond distance *regardless of the tensor orientations chosen*; we conclude that bond lengths equal to or greater than 2.9 Å are inconsistent with our data. Both simulations also involved a 25-Hz spinning speed offset from the exact rotational resonance condition and a 140-Hz (fwhm) Lorenzian line shape.

Measurement of the spectral line shape as a function of spinning speed yielded the spectra displayed in Figure 3. The top spectrum represents the high-speed limit, in which the sidebands are small and outside the range of all the centerbands. The central three speeds (8.61, 7.81, and 7.16 kHz) were chosen so as to match the spinning speed to the difference

Table I: Chemical Shift Parameters of Reactants and Enzyme-Bound Products[a]

species	σ_{iso}	σ_{11}	σ_{22}	σ_{33}	δ	η
enzyme–Ib–ATP						
II	53	−35	89	105	−88	0.18
X–O–PO_3^{2-}	−3	−68	−32	91	94	0.38
β-ADP	−8	−79	−22	78	85	0.67
α-ADP	−14	−109	0	66	−95	0.69
free inhibitors						
Ia (heptyl)	36	−27	25	110	74	0.70
Ib (methyl)	34	NA	NA	NA		
ATP–Mg–bipyridylamine						
α	−9	−123	12	83	−114	0.62
β	−17	−138	14	73	−121	0.49
γ	−6	−76	−24	82	88	0.59

[a] ^{31}P NMR chemical shift parameters for the phosphorus-containing substrates and products: ATP, (aminoalkyl)phosphinate inhibitors (Ia and Ib), and the enzyme-bound species ADP and the phosphorylated form of the inhibitor, II. All values are in ppm, except for η, which is unitless. Chemical shifts are relative to 85% phosphoric acid (with the convention that positive shifts are downfield). Parameters were determined from variable-speed MAS spectra by analysis of sideband intensities (Herzfeld & Berger, 1980). The shift elements for Ib were unavailable due to the amorphous nature of the sample. The shift tensor breadth, δ, and the asymmetry parameter, η, are defined as by the Spiess convention. In this convention, the three asymmetric tensor elements are designated by R_{xx}, R_{yy}, and R_{zz}, which are assigned such that $|R_{zz} - R_{iso}| \geq |R_{xx} - R_{iso}| \geq |R_{yy} - R_{iso}|$, $\delta = R_{zz} - R_{iso}$, and $\eta = (R_{yy} - R_{xx})/(R_{zz} - R_{iso})$. Note particularly the very large change in the inhibitor as it is bound with respect to both the isotropic shift value and the σ_{22} element.

in isotropic chemical shifts between the phosphinate and in turn each of the phosphates. This can be confirmed by noting that in each spectrum one of the −1 rotational sidebands from the three HPO_4^{2-} sites overlaps the phosphinate centerband. When $\omega_r/2\pi$ matched the difference for the phosphate ester and the phosphinate (7.16 kHz), a doublet line shape with a splitting of 150 Hz appeared on both lines. No such structure was apparent when ω_r matched the difference in isotropic shift for the phosphinate and either of the two ADP peaks. The lowest spectrum demonstrates that when the speed is further reduced, so that no sidebands are overlapping, the splitting is absent. This behavior established that the unidentified phosphate ester and the phosphinate inhibitor are dipolar coupled, and therefore in close proximity. In addition, the inhibitor is not coupled to ADP and therefore is spatially removed.

We have also determined the rate of magnetization transfer between the inhibitor and the phosphate at rotational resonance. Using the pulse sequence shown in Figure 2, we measured the rate of transfer on and off rotational resonance. Figure 6 shows two spectra taken at 0- and 3-ms mixing times illustrating the selective inversion and the final state after magnetization transfer. These data show a very rapid exchange of magnetization between the two sites, indicating that they are strongly dipolar coupled. Figure 7 shows a magnetization transfer with a set of time points, plotted together with our simulations (see Discussion). Off rotational resonance (or on rotational resonance for the phosphinate with the ADP phosphates) we could not detect any magnetization transfer during the initial 5 ms. This result is consistent with the line-shape analysis, which did not evidence any coupling between the phosphinate and the ADP, and indicates that the phosphinate is probably more than 5 Å from the ADP. The rapid completion of the magnetization transfer between the phosphate ester and the phosphinate, together with the fact that it only occurs at the rotational resonance condition, indicates that it is due to dipolar coupling between the two sites

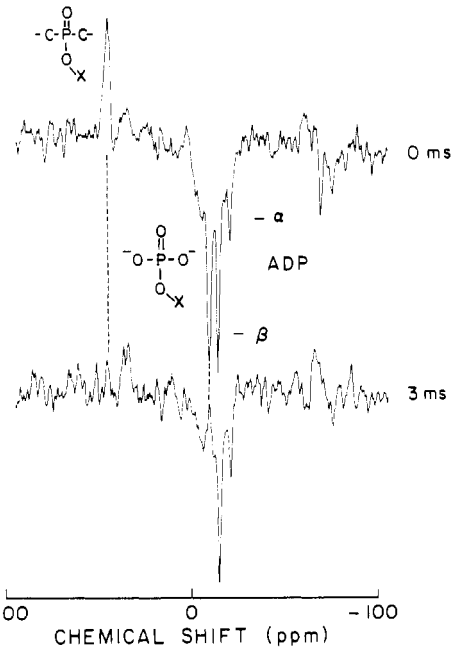

FIGURE 6: Magnetization-transfer spectra, taken with the pulse sequence illustrated in Figure 2, at 0- and 3-ms mixing times. The ADP peaks are distorted in intensity due to the selective inversion pulse. Note that the C–PO_2–C$^-$ and the X–PO_3^{2-} peaks are essentially nulled within 3 ms, while the ADP peaks persist.

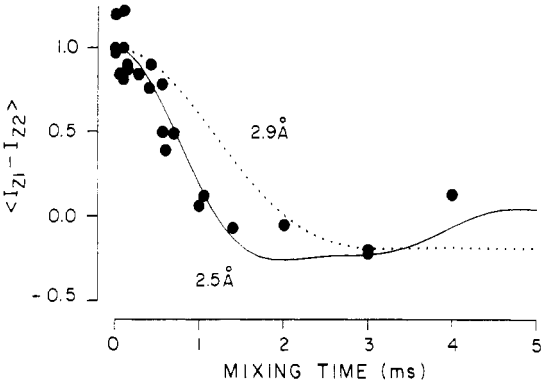

FIGURE 7: Magnetization exchange profile, consisting of differences of normalized amplitudes of the centerbands of the C–PO_2–C$^-$ and X–P–O_3^{2-} resonances, taken from spectra such as those shown in Figure 6. The solid line is a calculated decay based on a dipolar coupling of 1.26 kHz, corresponding to a P–P distance (in the P–O–P linkage) of 2.5 Å. We find good agreement between the data and the calculation for distances of 2.5–2.7 Å. The dashed simulation represents the best fit with a 2.9-Å distance regardless of the tensor orientations used; longer distances yield a less satisfactory agreement. From the poor quality of the 2.9-Å simulation, we conclude that a bond distance greater than 2.9 Å is unlikely.

and that they are strongly coupled. The numerical simulations of these spectra, presented under Discussion, offer strong evidence for the formation of a phosphoryl phosphinate following inhibition.

Discussion

Kinetic and Chemical Analyses of the Enzyme-Bound States of Ia and Ib. The slow-binding phosphinate inhibitor, Ib, forms an extremely stable complex with D-Ala-D-Ala ligase when incubated with Mg-ATP ($t_{1/2}$ = 17 days at 37 °C). Previously, the heptyl analogue, Ia; was shown to have a k_{rgn} = 2.3 × 10^{-5} s^{-1}, yielding a $t_{1/2}$ of 8.2 h (Duncan & Walsh, 1988). The complex formed with methyl inhibitor Ib is dramatically (50-fold) more stable than the complex formed by Ia. The initial K_i for Ib (methyl) and ligase is 140 μM, as

compared to the heptyl inhibitor, Ia, which has a K_i = 1.2 μM. The fact that this inhibitor complex is very long lived with high affinity made it very well suited for structural studies in the inhibited state. It is of obvious interest to understand the chemical basis for this remarkable stability on the enzyme and to test the viability of the proposed mechanism (Figure 1) in which phosphoryl transfer of the γ-PO_3 group of ATP to the phosphinate oxygen generates the phosphoryl phosphinate reaction intermediate analogue, II. If this mechanism is correct, the long lifetime would result from high-affinity binding and confer slow off rates to the tetrahedral adduct analogue of the normal reaction mechanism.

Previously, it was shown that the inhibition of *S. typhimurium* D-Ala-D-Ala ligase by inhibitor Ia in the presence of radiolabeled ATP leads to approximately 63% radiolabel in ATP and 37% in ADP and P_i (Duncan & Walsh, 1988). This study also reported that the enzyme retained 33% of the activity following gel filtration. In the current study, using Ib, we saw more complete hydrolysis of ATP, resulting in 76% ADP and P_i and 24% ATP. Thus, both the stability and the extent of reaction argued for the use of Ib. The issue of the existence of unreacted ATP on the enzyme after inhibition will be discussed in more detail later.

Since the proposed phosphoryl phosphinate II has not been detected after heat denaturation of the inhibited enzyme complex, presumably due to its hydrolytic lability, we investigated the inhibitor structure in the enzyme active site by NMR. ^{31}P MAS NMR has sufficient resolution and sensitivity to address these issues, with 50 mg ($\sim$1 μmol) of enzyme. Chemical shift tensor analysis of the enzyme-bound phosphorus species supported the proposed mechanism and the existence of the intermediate, II (shown in Figure 1). Measurement of the dipole coupling between two sites by an analysis of the line shapes and by observation of magnetization transfer at rotational resonance afforded unambiguous evidence of strong coupling between the phosphinate inhibitor and a phosphate species, and therefore of the spatial proximity of the two. The interpretation of the NMR data will be described in more detail in the following.

Chemical Shift Anisotropies. Previous solid-state NMR analysis of phosphates has delineated the spatial assignments of the three tensor components as follows: σ_{22} bisects the angle described by the two shortest P–O bonds, σ_{33} lies approximately 14° away from the longest P–O bond, and σ_{11} completes a Cartesian coordinate system (Herzfeld et al., 1978; Kohler et al., 1976; Un & Klein, 1989). Correlations between the particular values of the tensor elements and the P–O bond lengths and angles have been noted (Un & Klein, 1989). A salient point of the tensorial information available in the NMR of phosphates is that free inorganic phosphate is generally characterized by an overall tensor breadth, δ, of 45–75 ppm while pyrophosphates and organic esters of phosphates are typically broader, in the range of 65–110 ppm, and more asymmetric phosphates such as those in ATP are generally in the range of 100–120 ppm. Thus, we assign the resonance at −3 ppm, which has a breadth of 94 ppm, as either a polyphosphate or an organic ester of phosphate, but certainly not "free" inorganic phosphate. Furthermore, previous investigation allowed us to assign the probable spatial orientation of the tensor elements.

The inhibitor resonance exhibits dramatic changes in σ_{22} and σ_{iso} upon binding. On the basis of comparison of spectra of Ia and Ib taken in the solid state and in solution with a variety of solvents, we conclude that "environmental" noncovalent interactions are very unlikely to explain the large change in the isotropic shift of the inhibitor upon binding to the enzyme. We propose that a chemical modification would be more likely to explain these changes. In the case of phosphates and polyphosphates, changes in protonation state generally correlate with large changes in the tensor elements and the overall tensor breadth but relatively small changes in the isotropic position [see summary in Un and Klein (1989)]. In contrast, attachment of a phosphate to form a polyphosphate may cause a dramatic change in the isotropic shift (e.g., comparing the β- and α-phosphates in ATP). Thus, the chemical shielding parameters support the existence of intermediate II. We were unable to determine the complete tensor for the free methyl inhibitor, Ib, because of difficulties in crystallization; however, comparison of the tensor parameters for Ia in the free form and Ib bound to the enzyme suggests that the dramatic change in the isotropic chemical shift on binding is essentially localized in the σ_{22} element. We estimate that this element is aligned approximately along the ionized oxygen ligand, which we propose becomes phosphorylated upon binding. We emphasize however that this suggested assignment is *not* pivotal for any of the analyses or structural conclusions in this work.

Line-Shape Analysis. The induced splitting shown in Figures 3 and 5 is observed only at ω_r = 7.17 kHz. This observation indicates that the correct explanation for the splitting is a dipole coupling between these two sites. Such a coupling between two $I = {}^1/_2$ species would be averaged at an arbitrary spinning speed and reintroduced when $\delta = \omega_r$ (Andrew et al., 1966). We hasten to contrast the direct dipole coupling with the indirect dipole or J couplings sometimes observed for polyphosphates in solution NMR. The direct dipolar coupling, which is about 1 kHz, gives rise to a splitting of about 150 Hz, while the J coupling for adjacent ^{31}P atoms in ATP is approximately 20 Hz. Furthermore, the dipolar coupling is a manifestation of a through-space interaction and therefore a direct indicator of distance and not subject to through-bond or electronic effects.

The splitting in the line shape observed at rotational resonance was simulated to extract the magnitude of the dipolar coupling and therefore the through-space P–P distance in the P–O–P linkage. Simulations shown in Figure 5 show that the separation between the maxima, 150 Hz, is only consistent with a coupling greater than 800 Hz, or equivalently P–P distances less that 2.9 Å. These simulations depend on the dipolar coupling, the tensor parameters for the two sites, and the orientation of the two tensors relative to the internuclear axis. For the simulations shown, we employed a dipolar coupling of 1 kHz corresponding to 2.7 Å and a coupling of 800 Hz corresponding to a distance of 2.9 Å, together with the tensor orientations derived as described above. The simulation for 2.7 Å shown in Figure 5 is not a unique fit; the other simulations that arrive at the correct splitting employ *shorter* P–P distances and different tensor orientations. However, comparison with typical polyphosphate P–P distances of 2.85–3.3 Å (Calvo et al., 1968; Cini et al., 1984; Well, 1975) led us to consider the shorter distances to be unlikely. We emphasize that, regardless of the tensor orientations used, we cannot simulate this spectrum with P–P distances greater than 2.9 Å.

Magnetization-Transfer Experiments. For the magnetization-transfer experiments, as for the line-shape measurements, a dramatic dependence on ω_r was observed. No transfer is observed on the 5-ms time scale at other rotor speeds; this observation is proof that the transfer arises because of dipolar couplings between the two sites which are averaged by MAS

at arbitrary speeds. On a longer time scale (20 or 30 ms) we observe some magnetization transfer off rotational resonance. We have observed spin diffusion in ATP to have a similar rate (data not shown) so we attribute this off resonance transfer in the enzyme to spin diffusion. While a spin-diffusion measurement of this type would constitute evidence for coupling between the two sites, it is not a useful avenue for bond length determination, because of the complication of multispin interactions on this time scale.

As in the case of the line-shape simulations, the simulations of the magnetization-transfer rate depend on the dipolar coupling and the chemical shift tensor values and orientations. The simulations shown use distances of 2.5 and 2.9 Å and the tensor assignments as described above. The simulation with 2.5 Å yields excellent agreement with the data; distances up to 2.7 Å also agree adequately. However, we could not simulate these data well with P–P distances longer than 2.9 Å regardless of the tensor orientations used. It is possible to fit the curves with shorter P–P distances (as low as 2.3 Å) together with other tensor orientations, but we considered these distances to be unrealistic on the basis of comparison with P–P distances in a variety of polyphosphates (Calvo et al., 1968; Cini et al., 1984; Well, 1975).

Reproducibility and ATP Content. We comment that the tensor parameters as well as the evidence for dipolar coupling between the phosphinate and the phosphate ester were confirmed on two independent preparations of enzyme, together with two independent syntheses of inhibitor. At the moment it is not clear why one-fourth of the ATP remains bound to the enzyme–inhibitor complex and is not hydrolyzed, although the enzyme is fully inactivated. The ^{31}P NMR results are consistent with hydrolysis of the majority of the ATP to form ADP and phosphorylated inhibitor. The remaining ATP is apparently bound nonspecifically, giving rise to the broad underlying feature from 0 to −20 ppm. Some ATP bound to the enzyme could result if there were an equilibrium mixture of ATP, ADP, and inhibitor Ib and its phosphorylated form (II) present; however, we do not detect a resonance due to a "non-phosphorylated" form of inhibitor (i.e., Ib). The fact that the inhibited enzyme remains fully inactive following gel filtration would strongly argue against a dynamic equilibrium between the species Ib, II, ATP, and ADP. In addition, we note that the amount of ATP has been variable among three preparations of inhibited enzyme that we studied. It could be minimized by a washing procedure, described under Experimental Procedures, which did not affect the extent of catalytic inhibition. For these reasons we think it more likely that the broad ATP signal arises from an excess of ATP bound to the enzyme in a heterogeneous local environment. The presence of this signal did not interfere appreciably with the analyses of the sharp lines. It is of note that this situation differs from that of the heptyl-substituted inhibitor, Ia, which inhibits to a lesser extent and for which ATP predominated over ADP in the E–I complex (Duncan & Walsh, 1988).

Measurement of a P–P Distance in the P–O–P Linkage. The good agreement between the line-shape analysis and magnetization-transfer rate measurements lends great credibility to the existence of a covalent linkage between the inhibitor phosphinate and a PO_3 moiety and to the particular P–P length determined in this study. From the magnetization-transfer data and from the line-shape analysis, we conclude that the distance is 2.7 ± 0.2 Å; in both cases the preferred fit, on the basis of quality of simulation as well as chemical precedent, is produced with a distance of 2.6–2.7 Å. On the basis of our measurements, we would not rule out a distance as long as 2.9 Å, especially as a truly exhaustive study of possible systematic errors in this method has not been performed. Two potential sources of error in the experiment are the uncertainty in the anisotropic part of the J coupling between the two phosphorus atoms and the contribution of dynamic disorder in bond length to the averaged dipolar coupling. However, we believe that these errors are both likely to be small (ca. 0.1 Å). The estimated error range also includes a consideration of the fact that we do not know the exact tensor orientations.

To date, no complexes containing a phosphoryl–phosphinate linkage have been characterized, so we have no truly appropriate model compounds for this study. The closest analogues for comparison of P–P distances would be the polyphosphates. The specific distance measured in this study, 2.7 ± 0.2 Å, is rather surprising in light of previous distances for polyphosphates in ATP and various pyrophosphates, which fall in the range of 2.85–3.3 Å (Calvo, 1967; Cini et al., 1984; Well, 1975). From the above considerations of errors in this measurement, we suggest that P–P distances of 2.9–3.3 Å would be inconsistent with our data. The shorter P–O–P bond length found in our study, as compared with those of polyphosphates, is most likely related to bond angles at the bridging oxygen; it is also conceivable that the P–O bond length on the phosphinate is shorter than those found in polyphosphates. The bridging oxygen P–O–P angle might be more acute for the phosphoryl phosphinate than for polyphosphates because of conformational strain in the enzyme active site or, more likely, because of the reduced electrostatic repulsion when carbon atoms replace terminal oxygens on one site.

Conclusions

Using solid-state NMR measurements of ^{31}P chemical shift anisotropies and ^{31}P–^{31}P dipole couplings, we have demonstrated that inhibition by a slow-binding (aminoalkyl)phosphinate inhibitor of D-alanyl-D-alanine ligase is accompanied by phosphorylation at the phosphinate phosphorus by ATP. This inhibition mechanism mimics γ-PO_3^{2-} transfer in normal catalysis; the intermediate species is an isostere of the proposed tetrahedral adduct, D-Ala-PO_3^{2-}, formed in normal dipeptide formation. The tight binding of the transition-state analogue and the prodigiously long lifetime of this complex are explicable by the mechanism of a phosphoryl phosphinate stabilized against hydrolysis while held in the enzyme active site. This is the first conclusive demonstration of formation of a phosphoryl phosphinate in the active site of an enzyme, although it has been postulated in the slow-binding inhibition of glutamine synthetase by phosphinothricin and congeners. This phosphoryl-transfer mechanism may suggest a general strategy for design of slow-binding inhibitors in amide bond forming enzyme reactions.

Acknowledgments

We thank Valerie Copie, E. Ullian, and Dr. Ken Duncan for technical assistance, Dr. Sun Un for helpful discussions, and Dr. Malcolm Levitt for assistance with the computer simulations.

References

Andrew, E. R., Bradbury, A., & Eades, R. G. (1958) *Nature 182*, 1659.

Andrew, E. R., Bradbury, A., Eades, R. G., & Wynn, V. T. (1963) *Phys. Lett. 4*, 99–100.

Andrew, E. R., Clough, S., Farnell, L. F., Gledhill, T. D., & Roberts, I. (1966) *Phys. Lett. 21*, 505–506.

Calvo, C. (1968) *Inorg. Chem. 7*, 1345–1351.

Cini, R., Burla, M. C., Nunzi, A., Polidori, G. P., & Zanazzi, P. F. (1984) *J. Chem. Soc., Dalton Trans.*, 2467–2476.
Colanduoni, J. A., & Villafranca, J. J. (1986) *Bioorg. Chem. 14*, 163–169.
Columbo, M. G., Meier, B. H., & Ernst, R. R. (1988) *Chem. Phys. Lett. 146*, 189–195.
Copie, V., Faraci, W. S., Walsh, C. T., & Griffin, R. G. (1988) *Biochemistry 27*, 4966–4969.
Daub, E., Zawadzke, L. E., Botstein, D., & Walsh, C. T. (1988) *Biochemistry 27*, 3701–3708.
Duncan, K., & Walsh, C. T. (1988) *Biochemistry 27*, 3709–3714.
Griffin, R. G., Aue, W. P., Haberkorn, R. A., Harbison, G. S., Herzfeld, J. H., Menger, E. M., Munowitz, M. G., Olejniczak, E. T., Raleigh, D. P., Roberts, J. E., Ruben, D. J., Schmidt, A., Smith, S. O., & Vega, S. (1988) Magic-Angle Sample Spinning, *Physics of NMR Spectroscopy in Biology and Medecine* (Maraviglia, B., Ed.) pp 203–266, Soc. Ital. de Fisica, Rome.
Herzfeld, J., & Berger, A. E. (1980) *J. Chem. Phys. 73*, 6021–6030.
Herzfeld, J., Griffin, R. G., & Haberkorn, R. A. (1978) *Biochemistry 17*, 2711–2722.
Kohler, S. J., Ellett, J. D., & Klein, M. P. (1976) *J. Chem. Phys. 50*, 4451.
Knox, J. R., Liu, H., Walsh, C. T., & Zawadzke, L. E. (1989) *J. Mol. Biol. 205*, 461–463.
Logusch, E. W., Walker, D. M., McDonald, J. F., & Franz, J. E. (1989) *Biochemistry 28*, 3043–3051.
Lowe, I. J., (1959) *Phys. Rev. Lett. 2*, 285–287.
Manning, J. M., Moore, S., Rowe, W. B., & Meister, A. (1969) *Biochemistry 8*, 2681–2685.
Mariq, M. M., & Waugh, J. S. (1979) *J. Chem. Phys. 70*, 3300–3316.
Morrison, J. F., & Walsh, C. T. (1988) *Adv. Enzymol. Relat. Areas Mol. Biol. 61*, 201–301.
Park, J. (1958) *Symp. Soc. Gen. Microbiol., 8th*, 49–61.
Parsons, W. H., Patchett, A. A., Bull, H. B., Schoen, W. R., Taub, D., Davidson, J., Combs, P. L., Springer, J. P., Gadebusch, H., Weissberger, B., Valiant, M. E., Mellin, T. N., & Busch, R. D. (1988) *J. Med. Chem. 31*, 1772–1778.
Pines, A., Gibby, M. G., & Waugh, J. S. (1973) *J. Chem. Phys. 59*, 569–590.
Raleigh, D. P., Harbison, G. S., Neiss, T. G., Roberts, J. E., & Griffin, R. G. (1987) *Chem. Phys. Lett. 138*, 285–290.
Raleigh, D. P., Levitt, M. H., & Griffin, R. G. (1988) *Chem. Phys. Lett. 146*, 71–76.
Raleigh, D. P., Creuzet, F., Das Gupta, S. K., Levitt, M. H., & Griffin, R. G. (1989) *J. Am. Chem. Soc. 111*, 4502–4503.
Ronzio, R. A., Rowe, W. B., & Meister, A. (1969) *Biochemistry 8*, 1066–1075.
Rowe, W. B., Ronzio, R. A., & Meister, A. (1969) *Biochemistry 8*, 2674–2680.
Schaefer, J., & Stejskal, E. O. (1976) *J. Am. Chem. Soc. 98*, 1031–1033.
Un, S., & Klein, M. P. (1989) *J. Am. Chem. Soc. 111*, 5119–5124.
Walsh, C. T. (1989) *J. Biol. Chem. 264*, 2393–2396.
Well, H. F. (1975) *Structural Inorganic Chemistry*, Clarendon, Oxford.

N-Acetylimidazole Inactivates Renal Na,K-ATPase by Disrupting ATP Binding to the Catalytic Site†

José M. Argüello and Jack H. Kaplan*
Department of Physiology, University of Pennsylvania, Philadelphia, Pennsylvania 19104-6085
Received November 20, 1989; Revised Manuscript Received February 15, 1990

ABSTRACT: Treatment of renal Na,K-ATPase with *N*-acetylimidazole (NAI) results in loss of Na,K-ATPase activity. The inactivation kinetics can be described by a model in which two classes of sites are acetylated by NAI. The class I sites are rapidly reacting, the acetylation is prevented by the presence of ATP ($K_{0.5} \simeq 8\ \mu M$), and the inactivation is reversed by incubation with hydroxylamine. These data suggest that the class I sites are tyrosine residues at the ATP binding site. The second class of sites are more slowly reacting, not protected by ATP, nor reversed by hydroxylamine treatment. These are probably lysine residues elsewhere in the protein. The associated K-stimulated *p*-nitrophenylphosphatase activity is inactivated by acetylation of the class II sites only; thus the tyrosine residues associated with ATP binding to the catalytic center are not essential for phosphatase activity. Inactivated enzyme no longer has high-affinity ATP binding associated with the catalytic site, although low-affinity ATP effects (inhibition of phosphatase and deocclusion of Rb) are still present. The inactivated enzyme can still be phosphorylated by P_i, occlude Rb^+ ions, and undergo the major conformational transitions between the E_1 Na and E_2 K forms of the enzyme. Thus acetylation of the Na,K-ATPase by NAI inhibits high-affinity ATP binding to the catalytic center and produces inactivation.

The Na,K-ATPase (EC 3.6.1.3) is the plasma membrane enzyme that performs the transmembrane-coupled active transport of Na^+ and K^+ ions (Glynn, 1985; Kaplan, 1985; Norby, 1983). The biochemical activities catalyzed by the enzyme and their involvement in the associated transport reactions have been the focus of much work (Cantley, 1981; Kaplan, 1983). The enzyme subunit composition (Jorgensen, 1983, 1974b) and the primary sequence of the α subunit from several sources including torpedo (Kawakami et al., 1985),

† This work was supported by NIH HL-30315 and GM39500.
* To whom correspondence should be addressed.

0006-2960/90/0429-5775$02.50/0